ISSN: 0976-3031

Available Online at http://www.recentscientific.com

CODEN: IJRSFP (USA)

International Journal of Recent Scientific Research
Vol. 9, Issue, 4(B), pp. 25612-25618, April, 2018

International Journal of Recent Scientific Research

DOI: 10.24327/IJRSR

Research Article

EFFECTS OF RADIATION AND THERMAL SLIP ON HEAT TRANSFER ANALYSIS OF NON-NEWTONIAN FLUID FROM AN ISOTHERMAL SPHERE

Madhavi K[1]*., Nagendra N[2] and Raju GSS[1]

[1]Department of Mathematics, JNTUA College of Engineering, Pulivendula-516390, Andhra Pradesh, India
[2]Department of Mathematics, Madanapalle Institute of Technology & Science, Madanapalle, Andhra Pradesh, India

DOI: http://dx.doi.org/10.24327/ijrsr.2018.0904.1892

ARTICLE INFO

Article History:
Received 8th January, 2018
Received in revised form 21st February, 2018
Accepted 05th March, 2018
Published online 28th April, 2018

Key Words:

Eyring- Powell fluid, Radiation effect, Thermal Slip, Isothermal Sphere, Keller - Box finite difference scheme.

ABSTRACT

In this work, we focused on heat transfer analysis of Eyring Powell fluid from an isothermal sphere with the effects of radiation and thermal slip. The governing momentum and energy equations are transformed to nonlinear ordinary differential equations by use of a non-similarity transformation. These equations are described by numerically subject to physical applicable boundary conditions using the second order exact implicit finite difference Keller-box technique. The boundary layer conservation equations are parabolic in nature. The effects of Eyring Powell fluid parameter, Radiation parameter, Prandtl number and Thermal Slip on velocity and temperature profiles are discussed.

INTRODUCTION

The dynamics of non-Newtonian fluids has been a popular area of research because of its applications. Examples of such fluids include coal-oil slurries, shampoo, paints, clay coating and suspensions, grease, cosmetic products, custard and many others. The classical equations employed in simulating Newtonian viscous flows i.e., the Navier-Stokes equations fail to simulate a number of critical characteristics of non-Newtonian fluids. Hence several constitutive equations of non-Newtonian fluids has been presented over the past decades. The relationship between the shear stress and rate of strain in such fluids are very complicated in comparison in to viscous fluids. The viscoelastic features in non-Newtonian fluids and more complexities in the resulting equations. Besides all these challenges, several researchers even now are engaged in the flow analysis of non-Newtonian fluids. Hence several constitutive equations of non-Newtonian fluids have been presented over the past decades. Casson model, second- order Reiner-Rivlin differential fluid model, power-law Nano scale models, Eringen micro-morphic models, Jeffery's viscoelastic models.

The combination of natural and forced convection is known as dual convection and it is one of the main factors which affects the particle depositions. Dual convection flow plays a key role in electronic devices cooled by fans, atmosphere and ocean flows, drying of porous solid, solar power collectors, etc. In 1944, Eyring and Powell proposed a distinct model known as Powell-Eyring fluid model (Powell and Eyring, 1944). This model has certain benefits over another non-Newtonian model, because it is derived from molecular theory of gases rather than the experimental relation and turn into viscous (Newtonian) mode at high and low shear rates. Even though mathematically it is more complex but advantages of this fluid model overcomes its the mathematics. Heat, mass diffusion through Powell-Eyring fluid plays a vital role in different geophysical, natural and industrial problems. For example moisture and temperature distribution over agricultural pitches, environmental pollution, underground energy transport, etc. (Hayat *et al*, 2012) studied the steady flow of a Powell-Eyring

Corresponding author:* **Madhavi K
Department of Mathematics, JNTUA College of Engineering, Pulivendula-516390, Andhra Pradesh, India

fluid over a moving surface with convective boundary conditions. (Jalil *et al*, 2013) studied the flow and heat transfer of Powell-Eyring fluid over a moving surface in a parallel free stream. (Nagaraja *et al*, 2017) studied the laminar free convection boundary layer flow of Eyring Powell non-Newtonian fluid past a horizontal circular cylinder in the occurrence of magnetic field and Soret and Dufour effects. (Gaffar *et al*, 2016) investigates the nonlinear, steady boundary layer flow and heat transfer of an incompressible Eyring-Powell non-Newtonian fluid from an isothermal sphere with Biot number effects. (Malik *et al*, 2013) presented boundary layer flow of an Eyring Powell model fluid due to a stretching cylinder with variable viscosity. (Agbaje *et al*, 2017) explained this Paper he investigate the unsteady boundary-layer flow of an incompressible Powell-Eyring nanofluid over a shrinking surface. (Rehman *et al*, 2017) analyzed unsteady characteristics of magneto-hydrodynamic dual convection boundary layer stagnation point flow of Powell-Eyring fluid by way of cylindrical surface. (Patel and Timol, 2009) numerically examined the flow of Eyring - power fluids from a two-dimensional wedge. (Zueco and Beg, 2009) numerically studied the pulsatile flow of Eyring-Powell model. The effects of heat generation and thermal radiation on the fluid flow are taken into account. Radiation is the emission or transmission of energy in the form of waves or particles through space or through a material medium. Thermal radiation is a common synonym for infrared radiation emitted by objects at temperatures often encountered on Earth. Thermal radiation refers not only the radiation itself, but also the process by which the surface of an object radiates its thermal energy in the form black body radiation. Thermal radiation is generated when energy from the movement of charged particles within atoms is converted to electromagnetic radiation. (Gupta *et al*, 2013) used a vibrational finite element to simulate mixed convective-radiative micropolar shrinking sheet flow with a convective boundary conditions. (Ramachandra Prasad *et al*, 2007) analyzed the interaction of free convection with thermal radiation of a viscous incompressible unsteady flow past an impulsively started vertical plate with heat and mass transfer. (Agbaje *et al*, 2016) studied a numerical study of unsteady non-Newtonian Powell-Eyring nanofluid flow over a shrinking sheet with heat generation and thermal radiation. Muhammad (Tamoor *et al*, 2017) studied the primary focus of this paper was to numerically investigate the radiation and slip effects on the axi-symmetric laminar boundary layer flow of a viscous, incompressible fluid, electrically conducting fluid past a permeable stretching cylinder embedded in a porous medium. (Rapits, 1998) has analyzed the thermal radiation and free convection flow through a porous medium. (Chamka *et al*, 2001) have studied the radiation effects on free convection flow past a semi-infinite vertical plate with mass transfer. (Hayat *et al*, 2016) studied the combined effects of nonlinear thermal convection and radiation in 3D boundary layer flow of non-Newtonian Nano fluid are scrutinized numerically. (Nagendra *et al*, 2017) examined the nonlinear steady state boundary layer flow, Mathematical study of non-Newtonian nanofluid transport phenomena from an isothermal sphere, (Amanulla *et al*, 2017) explained Numerical Study of Thermal and Momentum Slip Effects on MHD Williamson Nanofluid from an Isothermal Sphere. (Nagendra *et al*, 2008) investigated Peristaltic motion of a power-law fluid in an asymmetric vertical channel. (Miraj *et al*, 2011) examined the effects of viscous dissipation and radiation on magneto-hydrodynamic free convection along a sphere with joule heating and heat generation. Further recent analyses include (Makinde and Aziz, 2010). (Gupta *et al*, 2014) used a vibrational finite element to simulate mixed convective radiative micropolar shrinking sheet flow with a convective boundary condition.

The objective of the present study is to examine 'Effects of Radiation and Thermal Slip on Heat Transfer Analysis of non-Newtonian Fluid from an Isothermal Sphere'. Numerical solutions for the velocity and the temperature distributions are obtained using a Keller-Box finite difference method.

Non-Newtonian Constitutive Eyring-Powell Fluid

In the present study a subclass of non-Newtonian fluids known as the Eyring-Powell fluid is employed flowing to its simplicity. The Cauchy stress tensor, in an Eyring-Powell non-Newtonian fluid takes the form:

$$\tau_{ij} = \mu \frac{\partial u_i}{\partial x_j} + \frac{1}{\beta}\sinh^{-1}\left(\frac{1}{C}\frac{\partial u_i}{\partial x_j}\right) \quad (1)$$

Where μ is dynamic viscosity, β and C are the rheological fluid parameters of the Eyring-Powell fluid model. Consider the second-order approximation of the $\sinh^{-1}$ function as:

$$\tau_{ij} = \sinh^{-1}\left(\frac{1}{C}\frac{\partial u_i}{\partial x_j}\right) \cong C\frac{\partial u_i}{\partial x_j} - \frac{1}{6}\left(\frac{1}{C}\frac{\partial u_i}{\partial x_j}\right)^3 \quad (2)$$

Where $\left|\frac{1}{C}\frac{\partial u_i}{\partial x_j}\right| << 1$

The introduction of the appropriate terms into the flow model is considered next. The resulting boundary value problem is found to be well-posed and permits an excellent mechanism for the assessment of rheological characteristics on the flow behavior.

Mathematical Flow Model

Consider the steady, laminar, two-dimensional, viscous, incompressible, buoyancy-driven convection heat transfer flow from an Isothermal Sphere embedded in an Eyring Powell non-Newtonian fluid. Fig.1 shows the flow model and physical coordinate system. Here x is measured along the surface of the sphere and y is measured normal to the surface, respectively and r is the radial distance from symmetric axes to the surface. r =a sin(x/a), 'a' is the radius of the sphere.

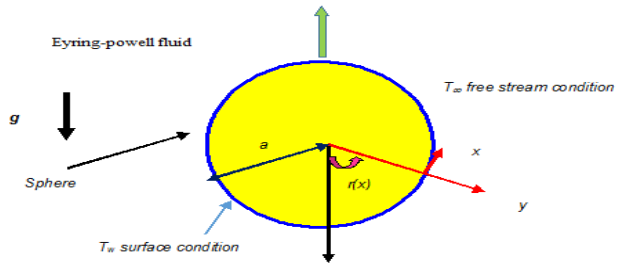

Fig 1 Physical model and coordinate system

The governing conservation equations can be written as follows:

$$\frac{\partial(ur)}{\partial x}+\frac{\partial(vr)}{\partial y}=0 \tag{3}$$

$$u\frac{\partial u}{\partial x}+v\frac{\partial u}{\partial y}=\left(\nu+\frac{1}{\rho\beta c}\right)\frac{\partial^2 u}{\partial y^2}-\frac{1}{2\rho\beta c^3}\left(\frac{\partial u}{\partial y}\right)^2\frac{\partial^2 u}{\partial y^2}+g\beta(T-T_\infty)\sin(\frac{x}{a}) \tag{4}$$

$$u\frac{\partial T}{\partial x}+v\frac{\partial T}{\partial y}=\alpha\frac{\partial^2 T}{\partial y^2}-\frac{1}{\rho c_p}\frac{\partial q_r}{\partial y} \tag{5}$$

Where u and v are velocity components in x and y directions respectively. The boundary conditions are prescribed at the surface and the edge of the boundary layer regime, respectively as follows:

$$At\ \ y=0\ \ :\ \ u=0,\ \ v=0,\ \ -K\frac{\partial T}{\partial y}=h_w(T_w-T)$$
$$As\ \ y\to\infty\ :\ u\to 0\ \ T\to T_\infty \tag{6}$$

Here T_∞ is the free stream temperature, k is the thermal conductivity, h_w is the convective heat transfer coefficient, and T_w is the convective fluid temperature. The stream function ψ is defined by

$$ru=\frac{\partial(r\psi)}{\partial y}\ \text{and}\ \ rv=-\frac{\partial(r\psi)}{\partial x} \tag{7}$$

And therefore, the continuity equation is automatically satisfied. In order to render the governing equations and the boundary conditions in dimensionless form, the following non-dimensional quantities are introduced.

$$\xi=\frac{x}{a},\ \ \eta=\frac{y}{a}Gr^{1/4},\ \psi=\nu\xi Gr^{-1/4}f(\xi,\eta)\theta=\frac{T-T_\infty}{T_w-T_\infty},\ Gr=\frac{g\beta(T_w-T_\infty)a^3}{\nu^3} \tag{8}$$

$$\varepsilon=\frac{1}{\mu\beta c},\ F=\frac{KK^*}{4\sigma^* T_\infty^3},\ \Pr=\frac{\nu}{\alpha},\ \delta=\frac{\upsilon^2}{2c^2a^4}Gr^{\frac{3}{2}}$$

In view of the transformations defined in the above equations, the boundary layer eqns. reduce to the following third order system of dimensionless partial differential equations of momentum and energy for the regime. Substituting eqns. (8) into the Eqns. (4)- (5), we obtain the following equations as

$$(1+\varepsilon)f'''+(1+\xi\cot\xi)ff''-\varepsilon\delta\xi^2 f''^2 f'''-f'^2+\frac{\sin\xi}{\xi}\theta=\xi\left(f'\frac{\partial f'}{\partial\xi}-f''\frac{\partial f}{\partial\xi}\right) \tag{9}$$

$$\frac{1}{\Pr}\left(1+\frac{4F}{3}\right)\theta''+(1+\xi\cot\xi)f\theta'=\xi\left(f'\frac{\partial\theta}{\partial\xi}-\theta'\frac{\partial f}{\partial\xi}\right) \tag{10}$$

The transformed dimensionless boundary conditions are as follows

$$At\ \ \eta=0,\ \ f=0, f'=0\ ,\ \theta=1+S_T\theta'(0)$$
$$As\ \ \eta\to\infty,\ f'\to 0,\ \ \theta\to 0 \tag{11}$$

Here primes indicate the differentiation with respect to η and $S_T=\frac{ah_w}{k}Gr^{\frac{1}{4}}$ is the thermal slip parameter. The wall thermal boundary condition in (11) relates to convective cooling. The skin rubbing coefficient and Nusselt number (heat transfer rate) can be defined using the transformations depicted in the above with the following expressions.

$$Gr^{-\frac{3}{4}}C_f=(1+\varepsilon)\xi f''(\xi,0)-\frac{\delta}{3}\varepsilon\xi^3\left(f''(\xi,0)\right)^3 \tag{12}$$

$$Gr^{1/4}Nu=-\theta'(\xi,0) \tag{13}$$

The location, $\xi \sqcup 0$, corresponds to the vicinity of the *lower stagnation point* on the sphere.

Since $\frac{\sin\xi}{\xi}\to\frac{0}{0}$ i.e. For this scenario, the model defined by equations(9)- (10) contracts to an ordinary differential boundary value problem:

$$(1+\varepsilon)f'''+f\,f''-(f')^2+\theta=0 \tag{14}$$

$$\frac{\theta''}{Pr}+f\,\theta'=0 \tag{15}$$

The general model is solved using a powerful and unconditionally stable finite difference technique introduced by (Keller, 1978). The Keller-box method has a second order accuracy with arbitrary spacing and attractive extrapolation features.

Numerical Solution

In this study, the efficient Keller-Box implicit difference method has been utilized to solve the general flow model characterized by equations with boundary conditions .This strategy was initially developed for low speed aerodynamic boundary layers and this system is produced by Keller and this frame work is developed by (Cebeci and Bradshaw, 1984).This strategy has been utilized in a various scope of modern multi-physical fluid flow issues. This technique remains among the most effective, adaptable and exact computational finite difference schemes employed in modern viscous fluid dynamics simulations. This method has been utilized broadly and effectively for more than three decades in a large spectrum of nonlinear fluid mechanics problems. Keller's techniques provides unconditional stability and rapid convergence for strongly non-linear flows. It includes four key stages, summarized below.

1. Reduction of the Nth order partial differential equation frame work to N first order equations
2. Finite difference discretization of reduced equations
3. Quasilinearization of non-linear Keller mathematical equations
4. Block-tridiagonal elimination of linearized Keller mathematical equations

Phase a: Reduction of the nth order partial differential equation system to N first order equations

New variables are introduced to Eqns. (9) - (10) subject to the boundary conditions are first written as a system of first order equations. For this purpose, we reset eqns. (9) - (10) as a set of simultaneous.

$$u(x,y)=f',\ v(x,y)=f'',\ t(x,y)=\theta' \tag{16}$$

These denote the variables for velocity and temperature respectively. Now Eqns. (9) - (10) are solved as a set of third order simultaneous differential equations:

$$f' = u \tag{17}$$

$$u' = v \tag{18}$$

$$\theta' = t \tag{19}$$

$$(1+\xi)v' + (1+\xi\cot\xi)\,fv - u^2 - \varepsilon\delta\xi^2 v^2 v' + \frac{\sin\xi}{\xi}s = \xi\left(u\frac{\partial u}{\partial\xi} - v\frac{\partial f}{\partial\xi}\right) \tag{20}$$

$$\frac{1}{\Pr}\left(1+\frac{4F}{3}\right)t' + (1+\xi\cot\xi)\,ft = \xi\left(u\frac{\partial s}{\partial\xi} - t\frac{\partial f}{\partial\xi}\right) \tag{21}$$

Where primes denote differentiation η. In terms of the dependent variables, the boundary conditions become:

$$\begin{aligned} &f = 0,\ u = 0,\ s = 1 \quad at\ \ \eta = 0 \\ &u \to 0, v \to 0,\ \ s \to 0 \quad as\ \ \eta \to \infty \end{aligned} \tag{22}$$

Phase b: Finite difference discretization of reduced boundary layer equations

A two - dimensional computational grid (mesh) is imposed on the $\xi - \eta$ plane as sketched in Fig.2. The stepping process is defined by:

$$\eta_0 = 0,\ \eta_j = \eta_{j-1} + h_j,\quad j = 1, 2, ...J,\ \eta_J \equiv \eta_\infty \tag{23}$$

$$\xi^0 = 0,\ \xi^n = \xi^{n-1} + k_n,\ \ n = 1, 2, ...N \tag{24}$$

Where k_n *and* h_j denote the step distances in the ξ (stream wise) and η (span wise) directions respectively

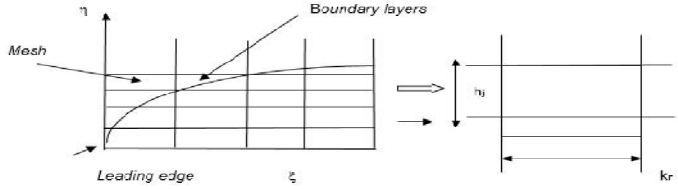

Fig 2 keller Box element and boundary layer mesh

If g_j^n denotes the value of any variable at $\left(n_j, \xi^n\right)$, then the variables and derivatives of equations. (25) (16)-(21) at $\left(n_{j-1/2}, \xi^{n-1/2}\right)$ are replaced by

$$g_{j-\frac{1}{2}}^{n-\frac{1}{2}} = \frac{1}{4}(g_j^n + g_{j-1}^n + g_j^{n-1} + g_{j-1}^{n-1}) \tag{25}$$

$$\left(\frac{\partial g}{\partial\eta}\right)_{j-\frac{1}{2}}^{n-\frac{1}{2}} = \frac{1}{2h_j}(g_j^n - g_{j-1}^n + g_j^{n-1} - g_{j-1}^{n-1}) \tag{26}$$

$$\left(\frac{\partial g}{\partial\xi}\right)_{j-\frac{1}{2}}^{n-\frac{1}{2}} = \frac{1}{2k^n}(g_j^n - g_{j-1}^n + g_j^{n-1} - g_{j-1}^{n-1}) \tag{27}$$

We now state the finite-difference approximation for equations (16) - (21) for the *mid-point* $\left(\eta_{j-1/2}, \xi^n\right)$, below

$$h_j^{-1}(f_j^n - f_{j-1}^n) = u_{j-\frac{1}{2}}^n \tag{28}$$

$$h_j^{-1}(u_j^n - u_{j-1}^n) = v_{j-\frac{1}{2}}^n \tag{29}$$

$$h_j^{-1}(s_j^n - s_{j-1}^n) = t_{j-\frac{1}{2}}^n \tag{30}$$

$$(1+\varepsilon)(v_j - v_{j-1}) + \alpha\frac{h_j}{2}v_{j-1}^{n-1}(f_j + f_{j-1}) - \alpha\frac{h_j}{2}f_{j-1}^{n-1}(v_j + v_{j-1}) - \frac{(\alpha+1)}{4}h_j(u_j + u_{j-1})^2 \tag{31}$$
$$-\frac{\xi^2\varepsilon\delta}{4}(v_j + v_{j-1})^2(v_j - v_{j-1}) + h_j\frac{B}{2}(s_j + s_{j-1}) + \frac{h_j A1}{4}(f_j + f_{j-1})(v_j + v_{j-1}) = [R]_{j-\frac{1}{2}}^{n-1}$$

$$\frac{1}{\Pr}\left(1+\frac{4F}{3}\right)(t_j - t_{j-1}) - \frac{h_j\alpha}{2}(t_j + t_{j-1})f^{n-1} + \frac{h_j A1}{4}(f_j + f_{j-1})(t_j + t_{j-1}) \tag{32}$$
$$-\frac{h_j\alpha}{4}(u_j + u_{j-1})(s_j + s_{j-1}) + \frac{h_j\alpha}{2}(u_j + u_{j-1})s^{n-1} - \frac{h_j\alpha}{2}(s_j + s_{j-1})u^{n-1}$$
$$+\frac{h_j\alpha}{2}(f_j + f_{j-1})t^{n-1} = [R_2]^{n-1}$$

Where, we have used the following abbreviations

$$\alpha = \frac{\xi^{n-\frac{1}{2}}}{k_n},\ \ B = \frac{\sin\xi}{\xi},\ A1 = 1 + \alpha + \xi\cot\xi$$

$$[R]_{j-\frac{1}{2}}^{n-1} = -h_j\left((1-\alpha+\xi\cot\xi)(fv)_{j-\frac{1}{2}}^{n-1} - (1-\alpha)(u^2)_{j-\frac{1}{2}}^{n-1} + (1+\varepsilon)(v^1)_{j-\frac{1}{2}}^{n-1} - \varepsilon\delta\xi^2(v^2)_{j-\frac{1}{2}}^{n-1}(v')_{j-\frac{1}{2}}^{n-1} + B(s)_{j-\frac{1}{2}}^{n-1}\right) \tag{33}$$

$$[R_2]_{j-\frac{1}{2}}^{n-1} = -h_j\left(\frac{1}{pr}\left(1+\frac{4F}{3}\right)(t')_{j-\frac{1}{2}}^{n-1} + \alpha(us)_{j-\frac{1}{2}}^{n-1} + (1-\alpha+\xi\cot\xi)(ft)_{j-\frac{1}{2}}^{n-1}\right) \tag{34}$$

The boundary conditions are

$$f_0^n = u_0^n = 0,\ s_0^n = 1,\ u_j^n = 0,\ v_j^n = 0,\ S_j^n = 0$$

Phase c: Quasilinearization of Non-Linear Keller Algebraic Equations

If we assume f_j^{n-1}, u_j^{n-1}, v_j^{n-1}, s_j^{n-1}, t_j^{n-1}, q_j^{n-1} to be known for the solution of 8J+8 equations for the solution of 6J+6 unknowns f_j^n, u_j^n, v_j^n, s_j^n, t_j^n, q_j^n $j = 0,1,2...J$. This non - linear system of algebraic equations is linearized by means of Newton's method as explained in (Keller, 1970) and (Subba Rao, 2016).

Phase d: Block-tridiagonal Elimination of Linear Keller Algebraic Equations

The linear system is solved using the block-elimination method, since it possess a block-tridiagonal structure consists of variables or constants, but here an interesting feature can be observed, namely that it consists of block matrices the complete linearized system is formulated as a block matrix system, where each element in the co-efficient matrix is a matrix itself. Then, this system is solved using the efficient Keller-box method. The numerical results are strongly influenced by the number of mesh points in both directions. After some trials in the η -directions (radial coordinate) a larger number of mesh points are selected whereas in the ξ - directions (tangential coordinate) significantly less mesh points are necessary. The numerical algorithm is executed in MATLAB on a PC. The method demonstrates excellent stability, convergence and consistency, as elaborated by Keller. Coupled boundary layer equations in a (ξ,η) coordinate system remain strongly nonlinear. A numerical method, the

Keller-Box implicit difference method, is therefore deployed to solve the boundary value problem defined by eqns. (9) - (10) with the boundary conditions (11).

NUMERICAL RESULTS AND DISCUSSION

Comprehensive solutions have been obtain and are presented in Figs. 3-10. The numerical issues includes two independent variables (ξ,η), two dependent fluid dynamic variables (f,θ) and 4 thermo-physical and body constrained control parameters, namely $\varepsilon, \Pr, F$ and S_T.

Figures 3- 4 illustrates the effect of Eyring-Powell fluid parameter ε, on velocity (f') and temperature (θ) distributions through the boundary layer regime. Velocity is significantly decreased with increasing ε at larger distance from the sphere surface owing to the simultaneous drop in dynamic viscosity. Conversely, temperature is consistently enhanced with increasing values of ε the mathematical model reduces to the Newtonian fluid as $\varepsilon \to 0$ and $\delta \to 0$. The momentum boundary layer equation in this case contracts to the familiar equation for Newtonian mixed convection from a sphere, viz.

$$f''' + (1+\xi\cot\xi)ff'' - \left(f'^2\right) + \frac{\sin\xi}{\xi}\theta = \xi\left(f'\frac{\partial f'}{\partial \xi} - f''\frac{\partial f}{\partial \xi}\right) \quad (35)$$

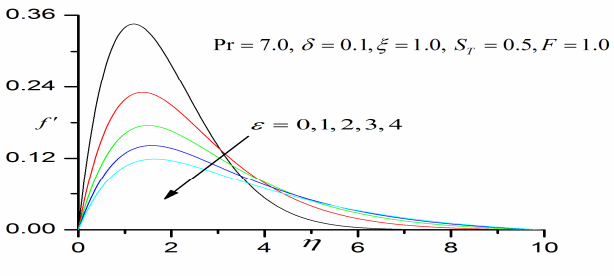

Fig 3 Influence of ε on velocity profiles

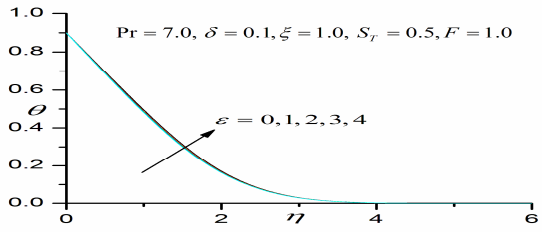

Fig 4 Influence of ε on temperature profiles

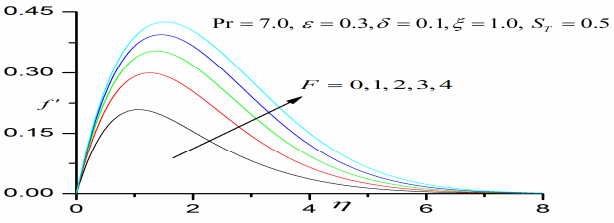

Fig 5 Influence of F on velocity

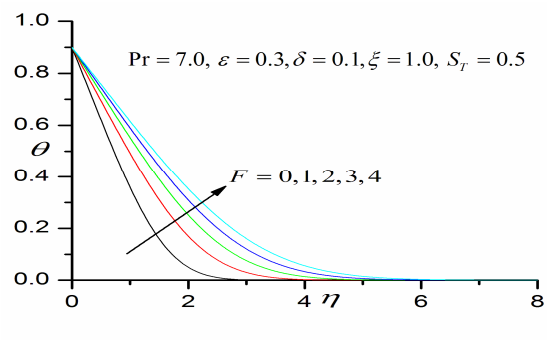

Fig 6 Influence of F on temperature profiles

Figures 5and 6 show the effects of radiation parameter F, It is observed that the velocity and temperature profiles are converges and close to the boundary layer when increasing the radiation parameter. The flow is accelerated and velocity is increased. The temperature profiles are also increases when increasing the radiation parameter.

Figures 7 and 8 depicts the effect of Prandtl number (Pr) on the velocity (f'), temperature (θ) distributions with transverse coordinate (η). Fig. 6 shows that with increasing Prandtl number there is a strong deceleration in the flow. The Prandtl number expresses the ratio of momentum diffusion rate to thermal diffusion rate. When Pr is unity both momentum and heat diffuse at the same rate and the velocity and thermal boundary layer thicknesses are the same. The monotonic decays in fig.7 are also characteristic of the temperature distribution in curved surface boundary layer flows.

Figures 9 and 10 illustrate the influence of the thermal slip S_T on the transient velocity and temperature. As S_T increases the velocity and temperature decreases. The cause the temperature buoyancy effects to decrease yielding a reduction in the fluid velocity. The increasing in the velocity and temperature profiles is accompanied by simultaneous reductions in velocity and temperature on boundary layer.

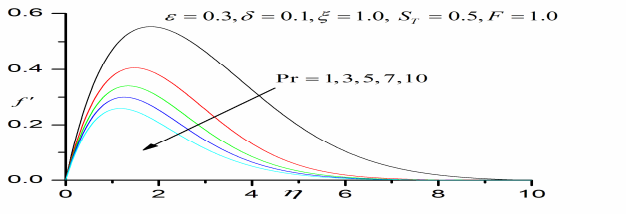

Fig 7 Influence of Pr on velocity profiles

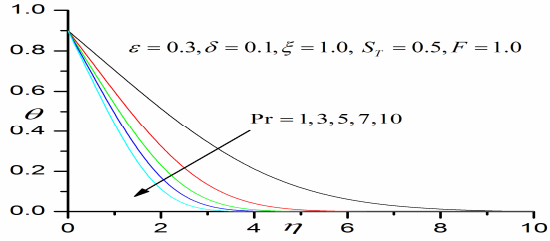

Fig 8 Influence of Pr on temperature profiles

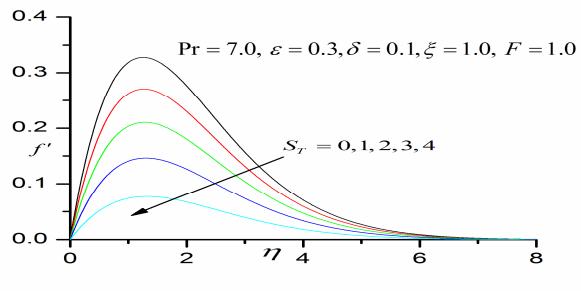

Fig 10 Influence of S_T on velocity profiles

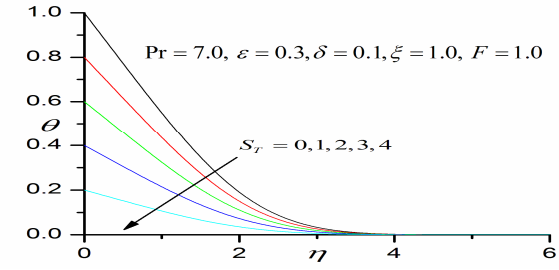

Fig 10 Influence of S_T on temperature profiles

CONCLUSIONS

Numerical solutions have been presented for the heat transfer analysis of non-Newtonian fluid from an Isothermal sphere with the effects of Radiation and Thermal Slip. The Keller-box implicit second order accurate numerical scheme has been utilized to efficiently solve the transformed, dimensionless velocity and boundary layer equations, subject to realistic boundary conditions. Excellent correlation with previous studies has been demonstrated testifying to the validity of the present code. The computations have shown that:

- Increasing Eyring-Powell fluid parameter (ε), reduces the velocity throughout the boundary layer, whereas it elevates temperature in the boundary layer.
- Enhancing the radiation parameter (F), increases velocity and temperature profiles throughout the boundary layer regime.
- Augmenting the Prandtl number (Pr), depresses the velocity and the temperature profiles throughout the boundary layer regime.
- Increasing the Thermal Slip (S_T), increases velocity and decreases the temperature profiles.

References

Powell, R.E., and Eyring, H. 1994. Mechanisms for the relaxation theory of viscosity. Nature, 3990, 30, 427-428.

Hayat, T., Iqbal, Z., Qasim, M and Bidat, O. 2012. Steady flow of an Eyring Powell fluid over a moving surface with convective boundary conditions, International *Journal of Heat and Mass Transfer*, 55,7, 1817-1822.

Jalil, M., Asghar, S., and Imran, S.M. 2013. Self similar solutions for the flow and heat transfer of Powell-Eyring fluid over a moving surface in a parallel free stream, *International Journal of Heat and Mass Transfer*, 65, 73-79.

Nagaraja, L., Sudhakar Reddy, M., and Suryanarayana Reddy, M. 2017. Magneto Hydrodynamic Effects on Non-Newtonian Eyring-Powell Fluid from A Circular Cylinder With Soret And Dufour Effects, *International Journal of Mathematical Archive*, 8, 6, 153-166.

Abdul Gaffar, S., Ramachandra Prasad, V., and Keshava Reddy, E. 2016. Non-Newtonian thermal convection of Eyring-Powell fluid from an isothermal sphere with biot-number effects, *International Journal of Industrial Mathematics*, 8,2, 131-146.

Malik, M.Y., Hussain, A., and Nadeem, S. 2013. Boundary layer flow of an Eyring Powell model fluid due to a stretching cylinder with variable viscosity, Scientia Iranica, Trans B: Mech Eng, 20, 2, 313-321.

Agbaje, T.M., Mondal, S., Motsa, S., and Sibanda, P. 2017. Unsteady boundary-layer flow of an incompressible Powell-Eyring nanofluid over a shrinking surface, Alexandria Engineering Journal, 56, 1, 81-91.

Rehman, K.U., Malik, M.Y., Bilal, S., and Bibi, M. 2017. Numerical analysis for MHD thermal and solutal stratified stagnation point flow of Powell-Eyring fluid induced by cylindrical surface with dual convection and heat generation effects, Results in Physics, *7*, 482-492.

Patel, M., and Timol, M.G. 2009. Numerical treatment of Powell-Eyring fluid flow using method of asympototic boundary conditions, Applied Numerical Mathematics, *59, 10*, 2584-2592.

Zueco, J., and Beg, O.A. 2009. Network numerical simulation applied to pulsatile non-Newtonian flow through a channel with couple stress and wall mass effects, *International Journal of Applied Mathematics, 5*, 1-16.

Gupta, D., Kumar, L., Beg, O.A. and Singh, B. 2013 Finite element simulation of mixed convection flow of micropolar fluid over a shrinking sheet with thermal radiation, Proc. IMechE. Part E: *Journal of Process Mechanical Engineering*, 2013.

Ramachandra Prasad, V., Bhaskar Reddy, N., and Muthukumara swamy, R.R. 2007. Radiation and mass transfer effects on two-dimensional flow past an impulsively started infinite vertical plate, *International Journal of Thermal Sciences*, 46,12, 1251-1258.

Agbaje, T.M., Mondal, S., Motsa, S.S., and Sibanda, P. 2017. Numerical study of unsteady non-Newtonian Powell-Eyring nanofluid flow over a shrinking sheet with heat generation and thermal radiation, Alexandria Engineering Journal, 56,1, 81-91.

Muhammad Tamoor, Shahzeb and Qamar Zaman, 2017. Radiation and slip effects on the axi-symmetric laminar boundary layer flow of a viscous, incompressible fluid, electrically conducting fluid past a permeable stretching cylinder embedded in a porous medium, *Alexandria Engineering Journal*, 90, 28-32.

Rapits, A. 1998. Radiation and free convection flow through a porous medium, Int. Comm. Heat Mass Transfer, 25, 289-295.

Chamkha, A.J., and Takhar, H.S., Soundlgekar, V.M., Radiation effects on free convection flow past a semi-infinite vertical plate with mass transfer, Chemical Engineering Journal. 84.

Hayat, T., Rashida, M., Imtiaza, M. and Alsaedi, A. 2016. the combined effects of nonlinear thermal convection and radiation in 3D boundary layer flow of non-Newtonian Nano fluid are scrutinized numerically, *Journal of Molecular Liquids*, 42,68-74.

Amanulla, C.H., Nagendr, N., Surya Narayana Reddy, M., Subba Rao, A., and Anwar Bég, O. 2017. Mathematical study of non-Newtonian nanofluid transport phenomena from an isothermal sphere, Frontiers in Heat and Mass Transfer, 8, 29, 1-13.

Amanulla, C.H., Nagendra, N., and Reddy M.S.N. 2017. Numerical Study of Thermal and Momentum Slip Effects on MHD Williamson Nanofluid from an Isothermal Sphere, *Journal of Nanofluids*, 6(6), 1111-1126

Nagendra, N., Subba Reddy, M.V., and Jayaraj, B. 2008. Peristaltic motion of a power-law fluid in an asymmetric vertical channel, *Journal of Interdisciplinary Mathematics*, 11(4), 505-519.

Miraj, M., Alim, M. A., and Andallah, L. S. 2011. Effects of viscous dissipation and radiation on magnetohydrodynamic free convection flow a long a sphere with joule heating and heat generation, Thammasat *Int. J. Science and Technology*, 16, 4, 52-64.

Makinde, O. D., and Aziz, A. 2010. MHD mixed convection from a vertical plate embedded in a porous medium with a convective boundary condition, *Int. J. Therm. Sci*. 49, 1813-1820.

Gupta, D., Kumar, L., Anwar, O., and Singh, B. 2014.

Finite element simulation of mixed convection ow of micropolar uid over a shrinking sheet with thermal radiation, Proc. IMechE. Part E*: J Process Mechanical Engineering*, 228, 61-72.

Keller, H. B. 1978. Numerical methods in boundary layer theory, Ann. Rev. Fluid Mech.10, 417-433.

Cebeci, T., and Bradshaw, P. 1984. Low speed aerodynamic boundary layers (frame work) Springer, New York.

Keller, H.B. 1970. A New Difference Method for parabolic problems, J. Bramble (Editor), Numerical Methods for partial Differential Equations, Acaemic press, New York, USA.

Subba Rao, A., Ramachandra Prasad, V., Nagendra, N., Bhaskar Reddy, N., and Anwar Beg, O. 2016. Non-Similar Computational Solution for Boundary layer Flows of Non-Newtonian Fluid from an inclined plate with Thermal slip, *Journal of Applied Fluid Mechanics*, 9, 2, 795-807.

How to cite this article:

Madhavi K *et al*.2018, Effects of Radiation And Thermal Slip on Heat Transfer Analysis of Non-Newtonian Fluid From An Isothermal Sphere. *Int J Recent Sci Res.* 9(4), pp. 25612-25618. DOI: http://dx.doi.org/10.24327/ijrsr.2018.0904.1892

****